

Using circularly polarized soft x rays to probe antiferromagnetically correlated Co/Cu multilayers

S. Stadler^{a)}

Department of Physics, Southern Illinois University, Neckers 483A, Carbondale, Illinois 62901

Y. U. Idzerda and J. Dvorak

Department of Physics and Astronomy, Montana State University, Bozeman, Montana 79717

J. A. Borchers

National Institute of Standards and Technology, Gaithersburg, Maryland 20899

(Presented on 6 January 2004)

X-ray resonant magnetic scattering was used to study the antiferromagnetic correlation between weakly coupled Co layers in a [Co(6 nm)|Cu(6 nm)]₂₀ multilayer. Half-order peaks were observed for standard specular $\theta-2\theta$ scans with the energy of the incident x rays tuned to the Co L_3 absorption edge. Three characteristic lengths were extracted from fits to the multicomponent 3/2-order diffuse spectrum: average correlated domain size, average correlated domain wall thickness, and average in-plane structural correlation length. © 2004 American Institute of Physics.

[DOI: 10.1063/1.1669311]

INTRODUCTION

Layered structures that possess giant magnetoresistive (GMR) properties have potential applications in field sensors and other devices that exploit spin-polarized currents. Much research has been done on structures composed of alternating ferromagnetic (FM) and nonmagnetic (NM) layers, which exhibit oscillations between FM and antiferromagnetic (AF) coupling between neighboring FM layers as a function of NM spacer layer thickness.¹⁻⁴ This oscillation in AF/FM coupling has been successfully described using the Ruderman-Kittel-Kasuya-Yosida theory⁵ and, equivalently, using a description in which quantum interference effects of the electrons in the spacer layer facilitate the oscillations.⁶ AF coupling is associated with large GMR effects due to spin dependent electron scattering at the interfaces; the resistance of the layer is maximized in zero applied field where the neighboring FM layers are antiferromagnetically aligned. As the applied field is increased to saturation, all of the FM layers align with the field and the spin dependent scattering, and thus the resistivity is reduced.⁷ A signature of the increasing degree of the AF coupling between multilayers is the tilting, i.e., the reduction of the “squareness” of the hysteresis loop.⁸ Consequently, the saturation field increases with increased degree of AF coupling which can be quantified as $-4J_i = H_s M t_f$, where J_i is the AF interlayer exchange coupling constant, H_s is the saturation field, M is the magnetization, and t_f is the spacer layer thickness.

The saturation field, H_s , for strongly coupled Co/Cu multilayers is around 10 kG, which is not readily accessible in applications.⁹ However, it is known that weakly coupled structures, such as Co/Cu multilayers with spacers on the order of 6 nm or greater, can exhibit significant (a few per-

cent) current-in-plane magnetoresistance with $H_s < 1$ kG.^{9,10} It is therefore beneficial to understand the physics of weakly coupled FM/NM multilayers.

The MR is defined by $MR(H) = [R(P) - R(H)]/R(P)$, where $R(P)$ is the resistance measured when the layers are aligned parallel to one another. $MR(H)$ for a strongly AF coupled Co/Cu multilayer is largest at zero applied field since alternating FM layers are antialigned and spin-dependent electron scattering is maximized. The MR decreases with applied field and is at a minimum when the field reaches the saturation value.⁷

As the spacer layer thickness is increased and the FM layers become more weakly coupled, the $MR(H)$ changes shape so that the maximum MR occurs near the coercive field H_c . An intriguing observation is that, for a pristine sample that has never been exposed to a magnetic field, the $R(0)$ is significantly larger (about double) than $R(H_c)$.⁹ Once the multilayer is exposed to H_c , the pristine $R(0)$ cannot be recovered by exposure to a field $-H_c$ or by demagnetization.^{10,11} It is the pristine $R(0)$ that will be the focus of the rest of this article.

It was found that antiferromagnetic correlations between domains in adjacent FM layers were responsible for the high pristine $R(0)$. This was accomplished by identifying half-order peaks in neutron scattering experiments, using either unpolarized¹² or polarized^{10,13} neutrons. Half-order peaks resulted from an AF superlattice structure with twice the period of the bilayer. Polarized neutron reflectivity (PNR) together with scanning electron microscopy with polarization analysis (SEMPA) unequivocally identified the AF correlation in the pristine multilayers.¹⁰ The half-order peaks disappeared after applying a magnetic field of magnitude H_c , and were not recovered after field cycling or demagnetization.

In this article we focus on a method that is complementary to PNR, soft x-ray resonant magnetic scattering (SXRMS). SXRMS is similar to PNR in that it measures the

^{a)} Author to whom correspondence should be addressed; electronic mail: sstadler@physics.siu.edu

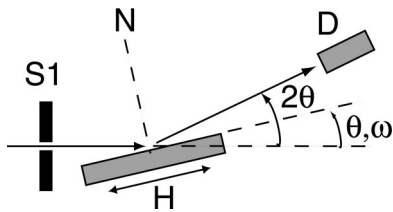


FIG. 1. The SXRMS scattering geometry. *N* is the sample normal, *S1* is an aperture that defines the incident beam dimensions, *D* is a slit/detector component, and *H* is the applied magnetic field.

momentum transfers Q_z and Q_x ; in our case, we measured the specular reflectivity as a function of incident angle (a $\theta-2\theta$ scan) at a resonant energy to obtain Q_z and, similarly, scanned the sample angle while keeping the detector stationary (conventional rocking scan) to obtain the diffuse spectrum and therefore Q_x (Fig. 1). An electromagnet was positioned such that we could apply a field simultaneously in the plane of the sample and the plane of incidence. SXRMS data, like PNR data, are sensitive to the size, orientation, and relative interlayer alignment of magnetic domains in buried layers.^{14,15} As is the case with PNR data, SXRMS data can yield information regarding chemical as well as magnetic roughness.¹⁵⁻¹⁸

EXPERIMENT

In this study, SXRMS was used to probe AF interlayer correlations between FM layers in a weakly coupled [Co(6 nm)|Cu(6 nm)]₂₀ multilayer. The multilayer was sputtered onto a 1 × 1 cm² Si substrate as described in detail elsewhere.¹⁹ The sample was identical to the samples used in the PNR study of Borchers *et al.*^{10,13} The XRMS data were acquired at the MSU-NSLS X-Ray Magnetic Circular Dichroism and Resonant Scattering Facility²⁰ at beamline U4B at the National Synchrotron Light Source at Brookhaven National Laboratory. The U4B monochromator is of the “Double Dragon” design, and is capable of producing highly circularly polarized (in excess of 90%) x rays in an energy range that spans 20–1350 eV.²¹

The first objective of this experiment was to use SXRMS to observe half-order specular reflections in a pristine [Co(6 nm)|Cu(6 nm)]₂₀ multilayer. The energy of the incident light was set to the Co *L*₃ absorption edge ($E = 778.9$ eV) and the degree of circular polarization was set to about 90%. These parameters were set to maximize the sensitivity of the incident photons to the magnetic state of the FM Co layers.

RESULTS AND DISCUSSION

A standard $\theta-2\theta$ scan was carried out before the pristine sample was subjected to an applied magnetic field. Half-order peaks were observed and are depicted in Fig. 2. The integer and half-order reflections are consistent with the simple Bragg reflection law: $m\lambda = 2d \sin \theta$, where m is the order number, λ is the wavelength of the incident light (15.9 Å), and d is the bilayer or AF superlattice period, i.e., 12 and 24 nm, respectively. The half-order peaks disappeared after field application ($H_s = 400$ G) and could not be recovered in

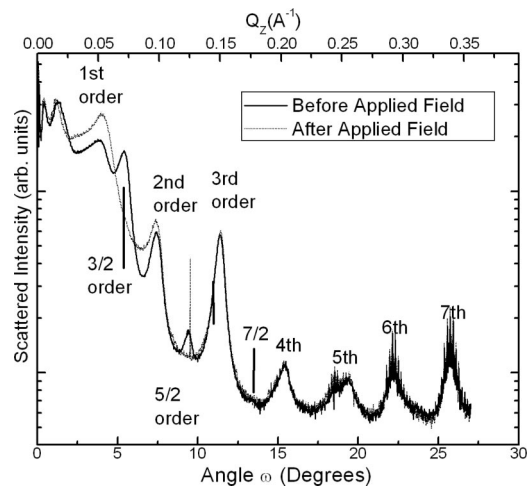


FIG. 2. Specular scans before and after the interlayer AF correlation was destroyed by the first field application.

the coercive state or by field cycling. It should be noted that 3/2- and 5/2-order reflections are easily observed, and the 7/2 order was barely discernable. The 1/2-order peak was not easily identified.

Rocking scans were measured at integer-order, half-integer-order, and off-order (between 3/2 and second-order) positions (Fig. 3). The spectra have been symmetrized and normalized to the intensity of the incident beam. The relative intensities of the half-order peaks can be used as a measure of the relative degree of AF correlation between the Co layers. The 3/2-order peak exhibits the most contrast between spectra measured before and after the first field application. The “after applied field” spectra in Fig. 2 were measured in remanence, i.e., the sample was still magnetized. Although this has an affect on the specular intensity, the diffuse scattering profile of the 3/2 peak could not be recovered in remanence or after field cycling demagnetization.

A conventional rocking scan spectrum is usually composed of two parts: a sharp specular peak and a broader diffuse background. The rocking scan centered on the 3/2-order peak before magnetic field application is somewhat

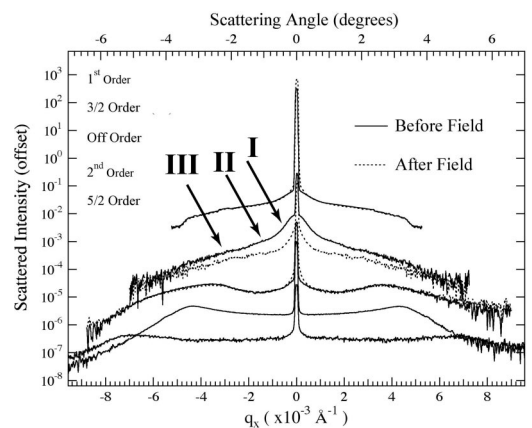


FIG. 3. Rocking scans centered on integer, half-integer, and off-order reflections before and after first field application. The scans are offset for clarity and are in the order indicated by the legend. Arrows point to the diffuse features I–III.

TABLE I. Correlation lengths extracted from fits of the three Gaussian components of the diffuse part of the 3/2-order rocking scan.

Region	Δq_x (\AA^{-1})	Γ (\AA) XRMS	Description	Γ (\AA) SEMPA
I	0.0418	7000	Domain size	5000–15 000
II	0.352	825	Domain wall	2000
III	2.22	130	Grain size	1000

more complicated. It is composed of at least four parts: (i) a sharp central specular peak; (ii) a diffuse portion which spans the range $\pm 0.7^\circ$ (region I), which is the most intense part of the diffuse spectrum; (iii) a part that spans $\pm 1.9^\circ$ (region II), and (iv) a broad, low intensity part which spans the entire angular range (region III).

In the case of a simple two-component rocking scan, the perpendicular and in-plane correlation parameters are proportional to the ratio of specular intensity to diffuse intensity and the full width at half maximum of the diffuse component, respectively.¹⁵ In order to extract the in-plane correlation lengths, we fit the various nonspecular components to a Gaussian, $\exp[-q^2/\Gamma^2]$, where q is the momentum transfer in the x direction and Γ is the fitted parameter which corresponds to the in-plane correlation length. The various fitted values for the correlation lengths are shown in Table I. After a saturating magnetic field (~ 400 G) was applied to the sample, the diffuse “lobes” corresponding to regions I and II disappeared. Although we cannot separate the contributions from the chemical and magnetic roughness to the diffuse spectrum, it is plausible that the disappearance of these features after the first field application are the direct result of the destruction of the pristine AF correlation between the Co layers. In order to assign a physical meaning to each of the extracted correlation lengths, we note that, in Ref. 10, three correlation lengths were identified in SEMPA images: (i) average domain size; (ii) average Neél-like domain wall width; and (iii) structural grain size (the corresponding values are listed in Table I). We therefore attribute the correlation length extracted from the fit of region I ($\sim 0.7 \mu\text{m}$) to the average size of the correlated domains. This value agrees well with that observed by SEMPA (0.5–1.5 μm). Note however, that the SEMPA estimates are considering the total domain size, whereas the XRMS data yield the average size of the correlated domains, putting the estimate of the latter towards the small range of the former.

Since the SEMPA measurements (Ref. 10) reveal that the AF correlation between adjacent Co layers even extends to such small features as domain walls, it should be possible to see the contributions from the domain walls in the magnetic rocking scans. We loosely attribute the diffuse intensity in Region II to AF correlated domain walls which, as is evident from the disappearance of region II intensity, become uncorrelated after field application. Our estimate of domain wall correlation length (825 \AA) is a little over a factor of 2 smaller than that estimated from SEMPA images (2000 \AA). It should be noted that an alternative explanation for the existence of the diffuse lobe of region II is possible: this diffuse intensity

could be the result of a second (smaller) average correlated domain size distribution in the multilayer. However, this was not directly observed in the SEMPA measurements.

Finally, the broadest component of this spectrum (region III) yields the structural correlation (130 \AA), which is smaller by a factor of 10 than the value observed in the SEMPA measurements. There are fundamental differences between the XRMS and SEMPA measurements. First, the incident x rays in the XRMS measurements were tuned to the Co L_3 absorption edge, making these measurements specific to Co, thus we are looking exclusively at the lateral correlation lengths of the Co layer. Second, in order to access the Co layer in SEMPA measurements, the overlayers were sputtered away with 2 keV Ar^+ ions. This additional processing may have changed the structural roughness of the surface. Although there is a distinct advantage of viewing domain structures using techniques such as SEMPA, this study accents the advantage of the element-specific and nondestructive probing capability of XRMS.

ACKNOWLEDGMENTS

The samples used in this study were furnished by J. Bass from Michigan State University. This work was supported by the Office of Naval Research and the National Institute for Standards and Technology. NSLS is supported by the Department of Energy.

- ¹S. S. P. Parkin, N. More, and K. P. Roche, *Phys. Rev. Lett.* **64**, 2304 (1990).
- ²S. S. P. Parkin, R. Bhadra, and K. P. Roche, *Phys. Rev. Lett.* **66**, 2152 (1991).
- ³S. S. P. Parkin, *Phys. Rev. B* **47**, 9136 (1993).
- ⁴J. W. Freeland, D. J. Keavney, D. F. Storm, I. L. Grigorov, J. C. Walker, M. G. Pini, P. Politi, and A. Rettori, *Phys. Rev. B* **54**, 9942 (1996).
- ⁵Y. Yafet, *J. Appl. Phys.* **61**, 4058 (1987).
- ⁶P. Bruno, *Europhys. Lett.* **23**, 615 (1993).
- ⁷M. N. Baibich, J. M. Broto, A. Fert, F. Nguyen van Dau, P. Eitenne, G. Creuzet, A. Friederich, and J. Chazelas, *Phys. Rev. Lett.* **61**, 2472 (1988).
- ⁸F. Nguyen van Dau *et al.*, *J. Phys. (Paris), Colloq.* **49**, C8-1633 (1988).
- ⁹W. P. Pratt, Jr., S.-F. Lee, J. M. Slaughter, R. Loloele, P. A. Schroeder, and J. Bass, *Phys. Rev. Lett.* **66**, 3060 (1991).
- ¹⁰J. A. Borchers *et al.*, *Phys. Rev. Lett.* **82**, 2796 (1999).
- ¹¹P. A. Schroeder, S.-F. Lee, P. Holoday, R. Loloele, Q. Yang, W. P. Pratt, Jr., and J. Bass, *J. Appl. Phys.* **76**, 6610 (1994).
- ¹²Ch. Rehm, F. Klose, D. Nagengast, B. Pietzak, H. Maletta, and A. Weidinger, *Physica B* **221**, 377 (1996).
- ¹³J. A. Borchers, J. A. Dura, C. F. Majkrzak, S. Y. Hsu, R. Loloele, W. P. Pratt, and J. Bass, *Physica B* **283**, 162 (2000).
- ¹⁴C. F. Majkrzak, *Physica B* **221**, 342 (1996).
- ¹⁵S. K. Sinha, E. B. Sorota, S. Garoff, and H. B. Stanley, *Phys. Rev. B* **38**, 2297 (1988).
- ¹⁶J. F. MacKay, C. Teichert, D. E. Savage, and M. G. Legally, *Phys. Rev. Lett.* **77**, 3925 (1996).
- ¹⁷J. W. Freeland, K. Bussman, and Y. U. Idzerda, *Appl. Phys. Lett.* **76**, 2603 (2000); J. W. Freeland, K. Bussman, Y. U. Idzerda, and C.-C. Kao, *Phys. Rev. B* **60**, R9923 (1999); J. W. Freeland, V. Chakarian, K. Bussmann, Y. U. Idzerda, H. Wende, and C.-C. Kao, *J. Appl. Phys.* **83**, 6290 (1998).
- ¹⁸R. M. Osgood III, S. K. Sinha, J. W. Freeland, Y. U. Idzerda, and S. D. Bader, *J. Appl. Phys.* **85**, 4619 (1999).
- ¹⁹J. M. Slaughter, W. P. Pratt, Jr., and P. A. Schoeder, *Rev. Sci. Instrum.* **60**, 127 (1996).
- ²⁰Y. U. Idzerda, V. Chakarian, and J. W. Freeland, *Synchrotron Radiat.* **10**, 6 (1997).
- ²¹C. T. Chen, *Nucl. Instrum. Methods Phys. Res. A* **256**, 595 (1987).